New Astronomy 36 (2015) 100–109

Contents lists available at ScienceDirect

New Astronomy

journal homepage: www.elsevier.com/locate/newast

Absolute and geometric parameters of the W UMa type contact binary V546 And

Birol Gürol [a,*], David H. Bradstreet [b], Abdullah Okan [a]

[a] Ankara University, Science Faculty, Dept. of Astronomy and Space Sciences, 06100 Tandoğan, Ankara, Turkey
[b] Eastern University, Dept. of Astronomy & Physics, St. Davids, PA 19087, USA

HIGHLIGHTS

- We present the first analysis of spectroscopic and photometric observations of V546 And.
- The orbital and physical parameters of the system were obtained.
- Our model describes V546 And as a W-type overcontact system.

ARTICLE INFO

Article history:
Received 16 July 2014
Received in revised form 20 October 2014
Accepted 22 October 2014
Available online 29 October 2014
Communicated by E.P.J. van den Heuvel

Keywords:
Stars: binaries: eclipsing
Stars: fundamental parameters
Technique: photometry & spectroscopy
Stars: individual (V546 And)

ABSTRACT

We present the results of our investigation on the geometrical and physical parameters of the W UMa-type binary V546 And from analyzed CCD (BVRI) light curves and radial velocity data. The photometric data were obtained in 2010 and 2011 at Ankara University Observatory (AUO) and the spectroscopic observations were made in 2010 at TUBITAK National Observatory (TUG). Light and radial velocity observations were analyzed simultaneously by using the Wilson–Devinney (2013 revision) code to obtain absolute and geometrical parameters. The system was determined to be a W-type W UMa system. Combining our photometric solution with the spectroscopic data we derived masses and radii of the eclipsing system to be $M_1 = 0.275\ \mathrm{M}_\odot$, $M_2 = 1.083\ \mathrm{M}_\odot$, $R_1 = 0.661\ \mathrm{R}_\odot$ and $R_2 = 1.229\ \mathrm{R}_\odot$. We finally discuss the evolutionary status of the system.

1. Introduction

The short-period ($P \sim 0^d.3830$) binary system V546 And (TYC2828-0018-1, $V = 11^m.23$, $\alpha_{2000} = 01^h51^m12^s.582$, $\delta_{2000} = +43°49'07''.61$) was reported under new discoveries by Nicholson and Varley, 2006 and classified as a W UMa (EW) type eclipsing binary system with light elements:

$$HJD(MinI) = 2451475.61807 + 0^d.3831 \times E \tag{1}$$

In the NSVS database[1] there are two stars whose id's are 3847677 and 3960604 but which are most likely the same system. In the database of the NSVS variables given by Hoffman et al. (2009) the system's id is 3847677 and the given orbital period is $0^d.38293$ with the amplitude $\Delta V = 0^m.421$ and classified as "Double Star".

The identification of this binary system in the Rotse-1 database is [GGM2006] 03960603 and the given parameters are: orbital period $P = 0^d.383036$, maximum light $V_{max} = 11^m.239$, amplitude $\Delta V = 0^m.517$, and distance of the system $d = 215$ pc, all based upon the light curve data in the Rotse-1 magnitude system (Gettel et al., 2006).

In this study we derive the absolute parameters for V546 And using photometric observations secured in 2010 and 2011 at the Ankara University Observatory (AUO) and radial velocity data obtained at the TUBITAK National Observatory (TUG) in 2010. Using published timings of minimum light we revised the light elements given in the literature within the framework of the well-known O–C method. In addition to the magnitudes in the standard system, we calculated the colors and amplitudes of the light variation in different filters.

2. Observations

2.1. CCD photometry

Observations of V546 And in BVRI bands were carried out in 2010 and 2011 with an Apogee ALTA-U47 (1024 × 1024) CCD photometric system attached to the 0.40 m Meade-LX200GPS tele-

* Corresponding author at: Ankara University, Science Faculty, Dept. of Astronomy and Space Sciences, 06100 Tandoğan, Ankara, Turkey.
E-mail address: gurol@ankara.edu.tr (B. Gürol).

[1] http://skydot.lanl.gov/nsvs/

http://dx.doi.org/10.1016/j.newast.2014.10.007
1384-1076/

Table 1
Observation log of V546 And.

Obs.Date	Number of Obs. (B V R I)	Observers
09/16/2010	341 + 341 + 341 + 341	GS
09/27/2010	189 + 189 + 189 + 187	YD, TO
09/13/2011	69 + 69 + 69 + 69	GS
10/19/2011	307 + 307 + 307 + 307	ZT

Observers: GS: G.Saral, YD: Y.Demircan, TO: T.Ozum, ZT: Z.Terzioğlu.

scopes of the AUO. The telescope was equipped with a standard Johnson UBVRI filter set with a field of view of $11'.3 \times 11'.3$. The exposure time for each image was varied according to the filter used (for B filter 25 s, V&R filters 15 s and I filter 17 s). TYC2828-2477-1 ($\alpha_{2000} = 01^h50^m53^s.041,\ \delta_{2000} = +43°47'54''.16$), TYC2828-2459-1 ($\alpha_{2000} = 01^h50^m41^s.642,\ \delta_{2000} = +43°50'35''.63$) and TYC2828-0825-1 ($\alpha_{2000} = 01^h51^m24^s.982,\ \delta_{2000} = +43°47'58''.77$) were used as comparison and check stars, which are located on the same frame of the CCD camera as V546 And from the FK5 (2000). Information regarding the observational log is given in Table 1 including the observers and the number of observations.

The photometric calibration of the raw CCD images was performed according to the standard method using IRAF[2] software. All CCD images were reduced by means of the IRAF package in the standard fashion. The aperture photometry package within IRAF was also utilized to reduce the observed images. The probable errors of the observations were estimated by using the difference between the magnitude of the check and the comparison stars, which are constant within $\pm0^m.022,\ \pm0^m.011,\ \pm0^m.010$ and $\pm0^m.010$ for B, V, R and I bands, respectively. Differential extinction corrections were found to be negligible, since the comparison star is very close to the variable. The data may be obtained from authors upon request.

The magnitude and color values for variable, comparison and check stars were obtained from the All-sky spectrally matched Tycho2 stars, Pickles and Depagne (2010) catalogue and are listed in Table 2. These were obtained by fitting UBVRI-ZY and u′g′r′i′z′ magnitudes, spectral types, and distances for 2.4 million stars, derived from synthetic photometry of a library spectrum that best matched the Tycho2 B_T, V_T, NOMAD RN, and 2MASS JHK2/S catalogue magnitudes.

2.2. (O–C) analysis

We collected a total of 14 timings of minimum light given in Table 3 to revise the light elements given by Nicholson and Varley (2006). We re-analyzed the published data by Nicholson and Varley (2006) and found that light elements of $HJD(MinI) = 2451475.806047 + 0^d.383039(49) \times E$ significantly reduce the scatter of the published timings. Because the system's orbital period and period variation are important for the remaining analysis we decided to determine new light elements for the eclipsing system. By using the light elements given in Kreiner's Times of Minimum website we calculated the O–C variation as shown in Fig. 1.

We emphasize that the brief time span of observations and limited number of times of minimum light constrain us from coming to firm conclusions regarding the period variation of the system. As seen, the first time of minimum light is a crucial datum for any conclusion. If it is discarded from the analysis, we then could perform a linear fit on the O–C variation to obtain the corrections on the epoch and period of the eclipsing system. Discarding the minima times that show large deviations from the linear trend, the derived coefficients are $(O-C) = -0.00000135121 \times E + 0.046826359125$ (see Fig.2). Using these parameters, we obtained new light elements given below:

$$HJD(MinI) = 2451475.66490(9) + 0^d.38301760(7) \times E \quad (2)$$

where the parentheses indicate the amount of uncertainty in the last digit which were taken from the errors obtained from the fitting parameters, and E is the epoch. However we discovered that by using the new light elements our observations made on different dates did not phase well with each other. Because of this we did not use the light elements given in Eq. (2) to construct phased light curves. Using different period search algorithms on only our observations we determined that the light elements given below are more suitable to construct the phased light curves for subsequent analysis.

$$HJD(MinI) = 2455854.32192(4) + 0^d.3830195(43) \times E \quad (3)$$

We believe that the system's period is changing on a short timescale. Because of this we conclude that we must include the first time of minimum light and analyze the entire (O–C) variation with different assumptions.

The variation can be modeled by a downward-facing parabola which signifies a period decrease. The main cause of such a period change is thought to be mass transfer between components and/or mass loss from the system. Additionally it is possible that we are seeing a portion of a periodic variation which can be explained by the light-time effect of a third body in the system and/or magnetic activity or superposition of those phenomena at the same time.

After modifying the accepted light elements and discarding the times of minimum light that diverged from the general trend, we fit a parabola (see Fig. 3) and determined the coefficients to be:

$$(O-C) = -2.689808157 \times 10^{-10}E^2 - 1.788321028 \times 10^{-6}E + 7.585476 \times 10^{-3} \quad (4)$$

where $R^2 = 0.9877$ is found for the coefficient of regression.

The secular decrease of the period possibly results from mass transfer from the more massive to the less massive components, or from mass and angular momentum loss from the system. Taking the quadratic term and the mass of the components (see Table 10) into account the degree of period variation can be calculated as $dP/dt = -5.130 \times 10^{-7}$ day/yr $= -0.0443$ s/yr which is typical for such W UMa type systems. This requires a mass transfer from the secondary to the primary component of $\Delta m_2/dt = -1.650 \times 10^{-7}\ M_\odot$/yr.

Assuming the O–C variation to be caused by a third-body we can calculate the time delay of any observed eclipse due to orbiting around a third-body. We have chosen Irwin's (1952, 1959) definition for the zero of the light-time effect and fit the O–C variation in the usual way.

To investigate the global behavior of the O–C diagram we manually fitted the required parameters and calculated $\sum(O-C)^2$ values. Using all of the times of minimum light the $\sum(O-C)^2$ values reached values of 0.00004 and 0.00003 for fits (Fig. 3: Periodic fit 1) and (Fig. 3: Periodic fit 2), respectively. The parameters obtained by the light-time fits are given in Table 4.

As is well known, the unknown mass m_3 (as a function of inclination) can be derived from the following third-order equation:

$$m_3^3 \sin^3 i - m_3^2 f(m_3) - 2m_3 m_{12} f(m_3) - m_{12}^2 f(m_3) = 0 \quad (5)$$

where m_{12} and m_3 are the masses (in solar units) of the eclipsing pair and the third body, respectively. The mass function $f(m_3)$ can be expressed by the elements of the orbital parameters of the third-body as

[2] IRAF is distributed by the National Optical Astronomical Observatories, operated by the Association of the Universities for Research in Astronomy, Inc., under cooperative agreement with the National Science Foundation.

Table 2
Magnitude and color values of the variable, comparison and check stars from "All-sky spectrally matched Tycho2 stars" by Pickles and Depagne (2010).

Star	B	V	R	I	J	H	K	$B-V$	Sp. type
V546 And	11.900	11.202	10.800	10.460	9.965	9.623	9.527	0.698	G5
TYC2828-2477-1	12.330	11.554	11.080	10.680	10.131	9.724	9.670	0.776	K0V
TYC2828-2459-1	12.710	12.272	12.000	11.750	11.468	11.308	11.201	0.438	F5V
TYC2828-0825-1	11.160	10.115	9.550	9.060	8.293	7.762	7.655	1.045	K1III

Table 3
Light minimum times and (O–C) residuals of V546 And. Based on the ephemeris: JD(pri.) = 2451475.61807 + 0.38301895E. The period is from Jerzy Kreiner's Times of Minimum website.

JD(Hel.+2400000)	Epoch	Method	Min.Type	(O–C)	Ref.
51475.61807	0	ccd	I	+0.00000	Nicholson and Varley (2006)
55456.36470	10393	BVRI	I	+0.03068	Gökay et al. (2012)
55456.55580	10393.5	BVRI	II	+0.03027	Gökay et al. (2012)
55467.47210	10422	BVRI	I	+0.03053	Gökay et al. (2012)
55799.35915	11288.5	ccd	II	+0.03166	Honkov et al. (2013)
55854.32190	11432	BVRI	I	+0.03119	Gürsoytrak et al. (2013)
55854.51360	11432.5	BVRI	II	+0.03138	Gürsoytrak et al. (2013)
56169.74207	12255.5	VR	II	+0.03526	Bradstreet, unpublished
56170.69458	12258	VR	I	+0.03022	Bradstreet, unpublished
56180.65542	12284	VR	I	+0.03257	Bradstreet, unpublished
56181.80409	12287	VR	I	+0.03218	Bradstreet, unpublished
56246.53219	12456	ccd	I	+0.03008	Honkov et al. (2013)
56262.61900	12498	V	I	+0.03009	Diethelm (2013)
56594.69500	13365	ccd	I	+0.02866	Nelson (2014)

$$f(m_3) = \frac{(m_3 \sin i)^3}{(m_{12}+m_3)^3} = \frac{1}{P_3^2}\left[\frac{173.15A}{\sqrt{1-e^2\cos^2\omega}}\right]^3 \tag{6}$$

where A is the semi-amplitude in days, P_3 is the period of the (O–C) curve in years, e is the eccentricity of the third-body orbit. Using Eq. (5) we can calculate the mass function $f(m_3)$ of the system. Using the light-travel time semi-amplitudes yields radius of the orbit of the contact system about its common center of mass with the third body. Combining this radius with the periods giving in Table 4 and assuming a mass of 1.358 $M_\odot$ (see Section 3) for the contact system, the third body should have a mass of 0.289 and 0.330 $M_\odot$ (with the assumption of a coplanar orbit) at a distance 9.93 and 8.03 AU from the contact system, respectively.

Because of the paucity of times of minimum light and the limited time scale of the published timings the analysis is speculative for V546 And. But we can say that all of the results obtained by the (O–C) analysis are possible reasons for the period change of the eclipsing system. Additionally the cyclic variations could be caused by strong magnetic activity of the contact system, with the behavior of variation of the light curve (the so-called O'Connell effect) of V546 And exhibiting that of a sinusoidal period modulation, according to theory of Applegate (1992). Bradstreet et al. (2013) showed that on their 2012 observations there was a clear indication of the O'Connell effect, i.e., different quadrature heights which are attributed to starspots. This also could likely explain the apparent scatter in their times of minimum light because the secondary eclipse was noticeably asymmetric. Asymmetric eclipses have been shown (Hargis et al., 2000) to skew times of minimum light by up to several minutes. But in the observations which were acquired in 2010 and 2011 we did not see any clear indication of such activity. This should be tested by observing the system in the future and analyzing it again as was done for the AU Ser system by Gürol (2005). When this is accomplished we expect to be able to more definitively explain the (O–C) variation.

2.3. Light and color curves

We derived the colors of the eclipsing system by converting all of the observed magnitudes to the standard system. Because we

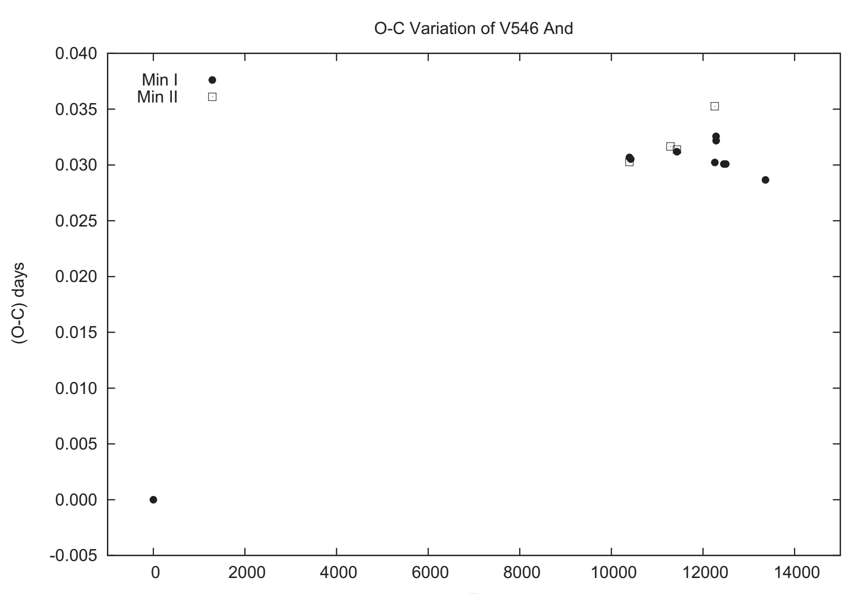

Fig. 1. (O–C) variation of V546 And. Based on the ephemeris: HJD(pri.) = 2451475.61807 + 0.38301895E.

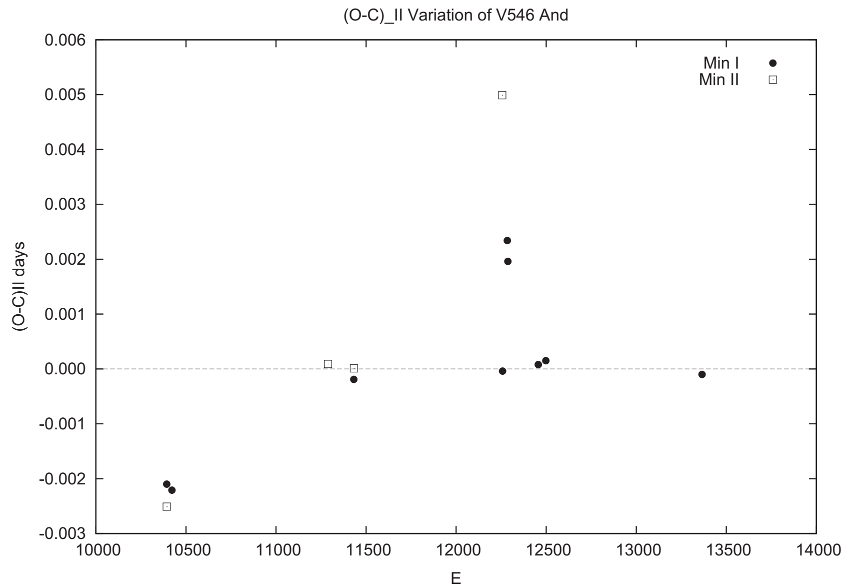

Fig. 2. (O–C) variation of V546 And.

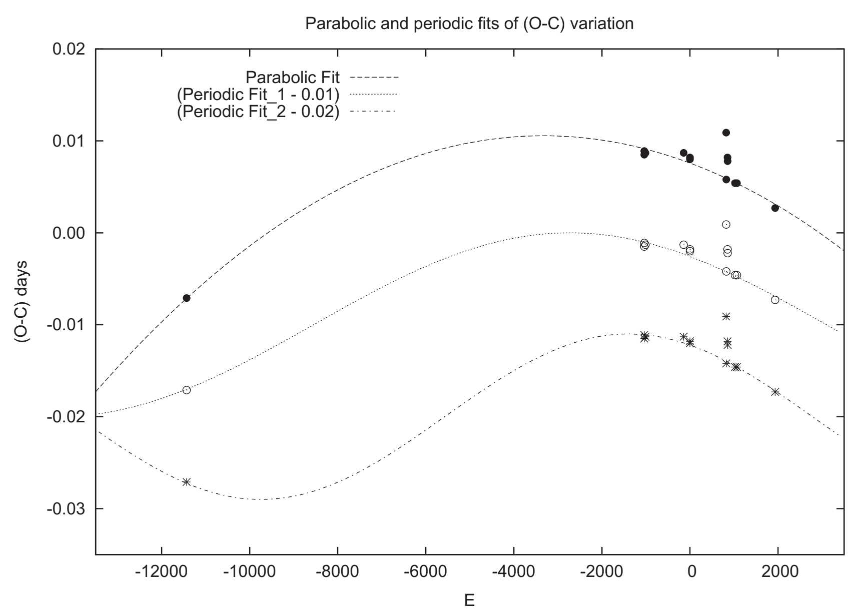

Fig. 3. Parabolic and two type of periodic fit on (O–C) variation of V546 And.

Table 4
The fit parameters used in Fig. 3.

Parameters	Values (Fit 1)	Values (Fit 2)
t_0 (HJD)	2455854.31392	24555854.31392
P (days)	0.38302036	0.38302036
A (days)	0.010	0.009
P_3 (yr)	24.43355058	17.512459
Starting epoch: t_3 (days)	same as t_0	same as t_0
Eccentricity: e	0.00	0.00
$\sum(O-C)^2$	0.00004	0.00003
$f(m_3)$	0.00869550	0.01233959
a_{12} (AU)	1.73781128	1.56403015
a_3 (AU)	8.19467240	6.46660813
m_3 $(M_\odot)$	0.289	0.330

obtained differential magnitudes of the eclipsing system as variable minus comparison on the observing nights, we prefer converting the comparison and check stars' observed magnitudes to the standard system and after that adding the determined standard magnitudes of the comparison star to the differential magnitudes in all filters. After correcting for atmospheric extinction, which was determined from the observations of the comparison star on each observing night, we obtained the standard magnitudes using the transformation coefficients that were derived for the same observing season at the AUO. The magnitudes and colors of the comparison and check stars are given in Table 5 which can be compared with the values given in Table 2. The observed light curves in the standard system are given in Fig. 4. From the comparison of the obtained $(B-V)$ colors with the values given in Table 2, we found

Table 5
Magnitude and color values for comparison and check stars in standard system.

Star	*B*	*V*	*R*	*I*	$B-V$	$V-R$	$V-I$
TYC2828-2477-1	12.115	11.408	11.010	10.656	0.707	0.397	0.752
TYC2828-2459-1	12.718	12.305	12.050	11.790	0.414	0.255	0.515
TYC2828-0825-1	11.056	10.079	9.579	9.102	0.978	0.500	0.976

small differences as $\Delta((B-V)_{AUO}-(B-V)_{Pickles}) = -0^m.069, -0^m.024$ and $-0^m.067$ for comparison and check stars, respectively.

As pointed out by Bradstreet et al. (2013) the primary minima are totally eclipsing. The secondary minima are also almost flat, with a small curvature, which can be attributed to the limb darkening on the eclipsed component. For systems which undergo complete eclipse, the derived orbital elements are much more reliable (Binnendijk, 1970). Since one of the components was totally eclipsed, we can determine the magnitude or light levels of the eclipsing and eclipsed components. Additionally, since the depth of the primary and secondary minima only differ slightly, we can say with certainty that the temperatures of the components must be nearly equal. It is important to note that, for light curves that show complete eclipses, the photometric mass ratios are usually very consistent with the spectroscopic mass ratio values (Terrell and Wilson, 2005).

We obtained the $(V-I)$, $(B-V)$ and $(V-R)$ color curves with respect to orbital phase that were calculated by averaging the observed magnitudes at 0.01 phase intervals and calculating the differences of the related magnitudes (Fig. 5). It is typical that for most W UMa-type binary systems, the color variation with respect

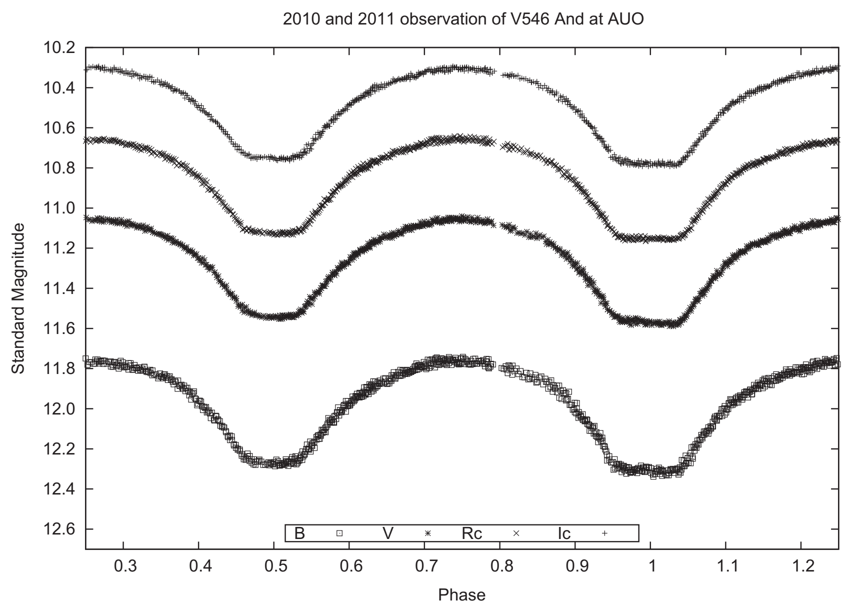

Fig. 4. BVRI light curve of V546 And.

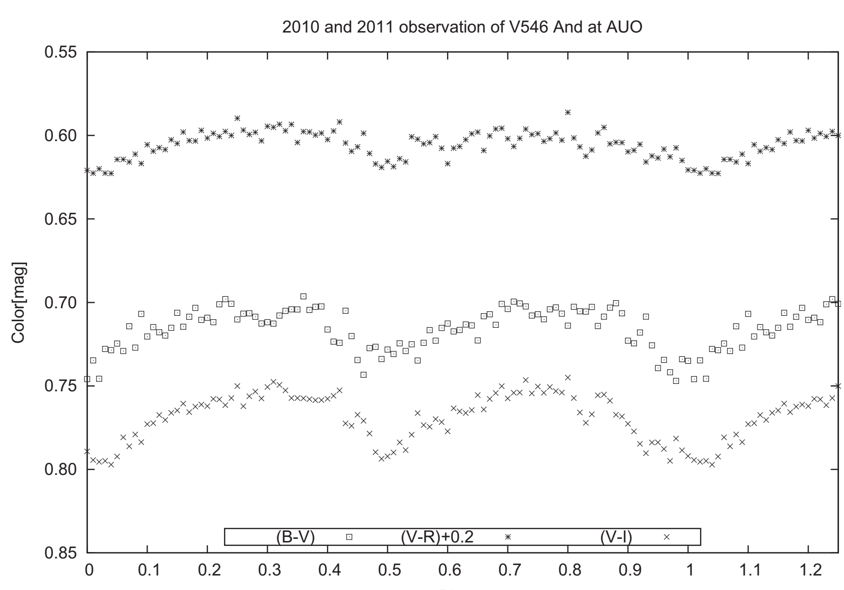

Fig. 5. Color curves of V546 And.

Table 6
Average of the magnitude and $(B-V)$ colors of V546 And on different phases.

Phase	$B \pm \sigma$	$V \pm \sigma$	$R \pm \sigma$	$I \pm \sigma$	$(B-V) \pm \sigma$
0.00	12.310 ± 0.014	11.573 ± 0.007	11.153 ± 0.005	10.781 ± 0.007	0.737 ± 0.015
0.25	11.766 ± 0.011	11.060 ± 0.005	10.665 ± 0.006	10.304 ± 0.006	0.706 ± 0.012
0.50	12.274 ± 0.008	11.543 ± 0.006	11.125 ± 0.005	10.751 ± 0.006	0.731 ± 0.010
0.75	11.765 ± 0.012	11.057 ± 0.008	10.656 ± 0.008	10.304 ± 0.006	0.708 ± 0.014

Table 7
Radial velocities of the primary and secondary components obtained by using the Broadening Function (BF24c) method published by Rucinski (1992) and Rucinski (2002) and programmed by Nelson (2005). σ is the standard deviation of the calculated radial velocities obtained for the suitable orders.

HJD		RV_1	$\pm\sigma$	RV_2	$\pm\sigma$
2400000+	Phase	(km/s)		(km/s)	
55521.21115	0.3034	+68.87	±14.50	−233.43	±06.90
55521.22259	0.3332	+33.61	±14.54	−220.58	±07.23
55521.41059	0.8241	−59.56	±07.16	+231.11	±13.45
55521.42202	0.8539	−52.78	±09.74	+193.11	±18.03
55522.16213	0.7862	−49.70	±14.36	+265.70	±12.71
55522.17357	0.8161	−45.75	±12.10	+240.14	±28.92
55522.18500	0.8459	−43.83	±17.26	+231.24	±27.55
55522.34112	0.2535	+32.19	±11.41	−287.50	±07.51
55522.35255	0.2834	+25.28	±08.23	−281.77	±04.19
55522.36398	0.3132	+11.20	±07.61	−270.66	±07.93
55522.46593	0.5794	−52.16	±08.72	+127.50	±11.52
55522.47738	0.6093	−58.24	±11.87	+169.08	±17.59
55522.48880	0.6391	−62.41	±12.73	+210.94	±08.42
55522.51467	0.7066	−58.90	±14.47	+251.63	±12.72
55522.52611	0.7365	−58.32	±13.71	+251.78	±16.55
55522.53754	0.7663	−60.33	±09.77	+250.72	±12.43
55522.54899	0.7962	−55.58	±10.12	+243.87	±18.79
55523.26074	0.6545	−61.62	±04.27	+224.90	±71.55
55523.27217	0.6844	−57.08	±06.04	+246.04	±25.88

Table 8
Colors and interpolated corresponding temperatures and errors obtained from the standard tables of Houdashelt et al. (2000) by adopting the assumption of dwarf stars and from the tables of Allen.

Color index	Temperature (K) (dwarf star)	Phase
$(B-V) = 0.737 \pm 0.015$	5468 ± 43	0.00
$(V-R) = 0.420 \pm 0.009$	5455 ± 48	0.00
$(V-I) = 0.792 \pm 0.010$	5434 ± 30	0.00
$(J-K)_{2MASS} = 0.439 \pm 0.033$	5576 ± 116*	0.54
$(J-H)_{2MASS} = 0.343 \pm 0.056$	5701 ± 360*	0.54

* Cox, 2000.

to the orbital phase does not vary very much, except near the primary minima. But as can be seen on Fig. 5 and in Table 6, the colors of V546 And change according to the orbital phase. At the primary and secondary minima the color is nearly the same $(B-V=0^m.73)$, which confirms that the temperatures of the components are nearly the same for this system.

2.4. Spectroscopy

Spectroscopic observations were obtained with the Turkish Faint Object Spectrograph Camera (TFOSC) attached to the 1.50 m telescope on November 20, 21, and 22, 2010. Further details on the telescope and the spectrograph can be found at http://www.tug.tubitak.gov.tr. The wavelength coverage of each spectrum was 3850–9120 Å in 11 orders, with a resolving power of 7000 at 6563 Å. We also obtained a high S/N spectrum of the HD12929 ($v_r = -14.64$ km/s, K2 III) and HD14969 ($v_r = -27.80$ km/s, K3 III) for use as templates in deriving the radial velocities of the binary.

We took a total of 19 spectra using an exposure time of 900 s. Bias subtraction and flat-field correction were made with standard IRAF procedures. The spectra were extracted using procedures from the IRAF package noao.imred.echelle. Wavelength calibration was performed using a Fe–Ar comparison lamp taken during the same observing run. $\Delta\lambda$ values are different for the 11 orders and changing between 0.288 and 0.751 Å/px. The velocity dispersion was changing between 22 and 27 km/s/px for different orders.

The exposure times given for the observations of V546 And are nearly 2.7% of the orbital period and this is slightly longer than the recommended values given by Hilditch (2001) (1–2% of the orbital phase). The heliocentric correction was applied with the RVCORR and DOPCOR tasks of the IRAF packages ASTUTIL and ECHELLE. Radial velocities were determined by using the Broadening Function (BF24c) method published by Rucinski (1992) and Rucinski (2002) for suitable orders. All of the velocities obtained from velocity standards were averaged and used to calculate the standard errors on the velocities. The derived radial velocities of the components are given in Table 7.

According to the radial velocity curves, we confirm the system to be a W-type W UMa system, i.e. the larger, more massive component has the lower surface temperature but contributes more overall brightness to the eclipsing system. It is this larger, cooler and more massive star that is eclipsed during the secondary minima.

3. Light Curve analysis

The Wilson and Devinney (Wilson and Devinney, 1971; Wilson, 1978; Wilson, 1979; Wilson, 1990; Wilson and Van Hamme, 2007) method was applied to solve the light curves of V546 And. We used the 2013 revision of the program which operates under the interface of MS Excel Software, programmed by B. Gürol for Windows. The method used assumes the stellar surfaces to be equipotentials and computes the light curves as a function of the following parameters: the orbital inclination i, surface potentials $\Omega_{1,2}$, flux-weighted average surface temperatures $T_{1,2}$, mass ratio $q = m_2/m_1$, normalized monochromatic luminosities $L_{1,2}$, limb-darkening coefficients $x_{1,2}$, gravity darkening exponents $g_{1,2}$, and bolometric albedos $A_{1,2}$. In this paper, the subscripts 1 and 2 refer to the primary (hotter, less massive) and secondary (cooler, more massive) components, respectively.

In order to obtain an accurate measure of the average temperature for the system, we used the Two Micron All Sky Survey (2MASS, Skrutskie et al., 2006) J-, H-, and K-band magnitudes. For V546 And, $J = 9.966 \pm 0.022$, $H = 9.623 \pm 0.028$, and $K = 9.527 \pm 0.024$. These values were taken simultaneously at phase 0.54, where the hotter and lower mass component was almost directly in front of the cooler one. Because the colors of the system (Fig. 5) do not vary at the primary and secondary minima, we can take the temperature values at these minima as an initial input value in the light curve analysis. The color indices computed in the light curve analysis and the corresponding temperatures and their errors interpolated from the standard tables

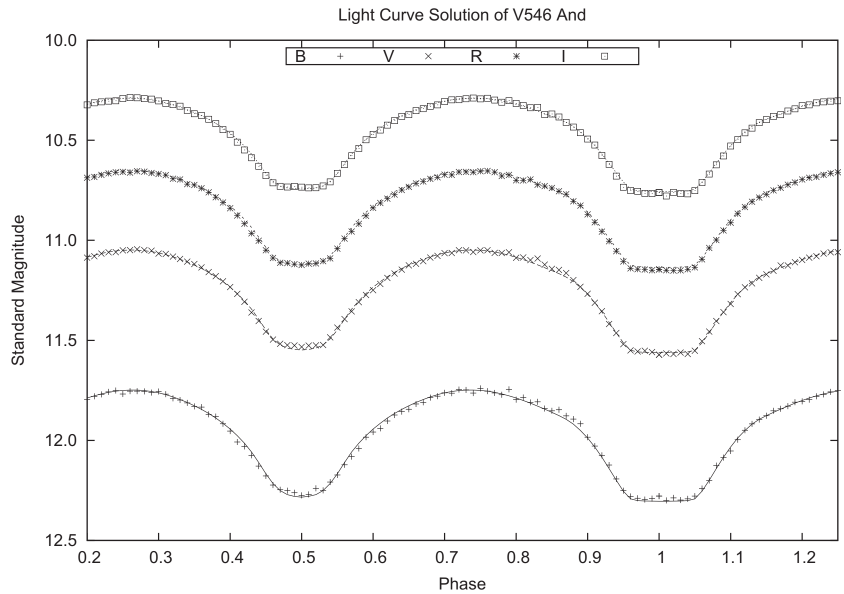

Fig. 6. The observational and theoretical light curves of V546 And. The symbols represent the observational data for BVRI filters and the lines the theoretical light curves for over-contact mode. The observations averaged by 0.01 phase intervals.

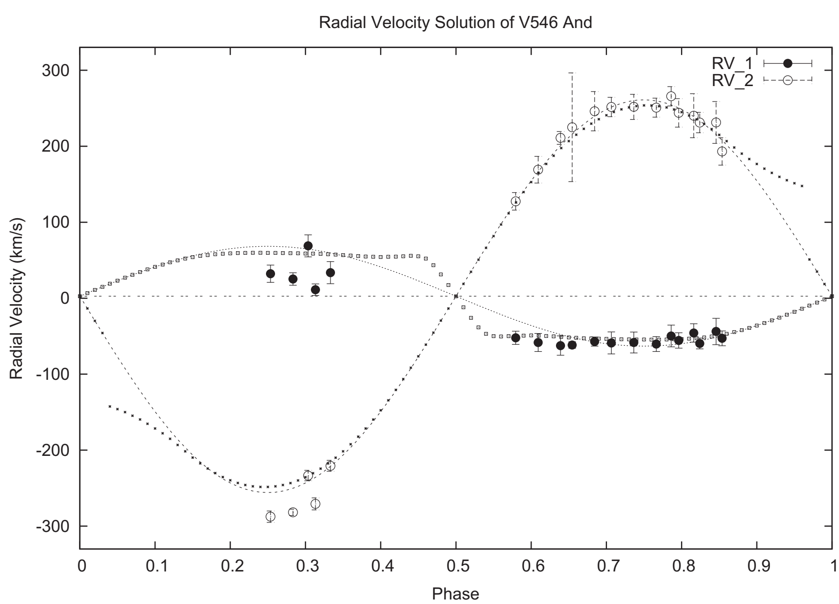

Fig. 7. The observational and theoretical radial velocity curves of V546 And. The curves are computed and circles are the observational data. Because of some shifting problems some of the data near the phase 0.25 were not used in the analysis.

of Houdashelt et al. (2000) and Allen's Astrophysical Quantities (Cox, 2000) are given in Table 8. For the primary minima nearly all of the colors give same temperature values which is indicative that it is the temperature of the cooler component in the absence of interstellar reddening.

The distance to the system is given by Gettel et al., 2006 as 215 pc, and if this distance is correct, the system's magnitudes/colors must be affected by the interstellar medium. The spectral type of the system was obtained by using the cross correlation function (CCF) found in the IRAF with respect to different types of comparison spectra. By using this method we determined that the hotter component's spectral type is located between F5 and F7. We choose F6 for the hotter component where the temperature corresponding to the spectral type is found as $T_1 = 6517$ K given by Cox (2000).

The Period–Color relation given by Wang (1994), under the assumption that the components in a contact binary system are formed from almost normal hydrogen-core-burning stars that obey the mass–radius relation for main sequence stars, predicts that the intrinsic color index can be written as:

$$(B - V)_0 = 0.077 - 1.003 logP(day) \quad (7)$$

where P is the orbital period in days. For this equation, the given correlation coefficient to the fit by Wang (1994) is only 0.78. This indicates that there is considerable scatter to the fit when compared to the actual observed data points. Using the period obtained in our

Table 9
The light and radial velocity curve solutions of V546 And. Assumed parameters are marked with asterisk, *.

Parameters	BVRI	$\pm\sigma$	Parameters	BVRI	$\pm\sigma$
a ($R_\odot$) =	2.458	0.022	$L_1(B)/L_{Tot.}$ =	0.26325	0.01001
V_γ (km/s) =	2.611	0.013	$L_1(V)/L_{Tot.}$ =	0.25134	0.00716
K_1 (km/s) =	−258.31	13.49	$L_1(R)/L_{Tot.}$ =	0.24534	0.00599
K_2 (km/s) =	65.81	3.24	$L_1(I)/L_{Tot.}$ =	0.24090	0.00523
i (°) =	86.071	0.271	$L_2(B)/L_{Tot.}$ =	0.73675	–
T_1 (K) =	6517*		$L_2(V)/L_{Tot.}$ =	0.74866	–
T_2 (K) =	6240	4	$L_2(R)/L_{Tot.}$ =	0.75466	–
$q = m_2/m_1$ =	3.9367	0.0114	$L_2(I)/L_{Tot.}$ =	0.75910	–
$A_1 = A_2$ =	0.50*	–	r_1 (pole) =	0.26080	0.00033
$g_1 = g_2$ =	0.32*	–	r_1 (side) =	0.27310	0.00038
x_1 (bolo) =	0.642*	–	r_1 (back) =	0.31658	0.00070
x_2 (bolo) =	0.647*	–	r_2 (pole) =	0.48019	0.00104
y_1 (bolo) =	0.240*	–	r_2 (side) =	0.52207	0.00152
y_2 (bolo) =	0.221*	–	r_2 (back) =	0.54990	0.00202
$\Omega_1 = \Omega_2$ =	7.64244	0.01337	$(RV_1)\sum(\text{O–C})^2$ =	2.6170	–
Ω_{in} =	7.83109	–	$(RV_2)\sum(\text{O–C})^2$ =	2.6619	–
Ω_{out} =	6.32855	–	$(B)\sum(\text{O–C})^2$ =	0.00972	–
Fillout:$f_1 = f_2$ =	12.56%	–	$(V)\sum(\text{O–C})^2$ =	0.00531	–
			$(R)\sum(\text{O–C})^2$ =	0.00505	–
			$(I)\sum(\text{O–C})^2$ =	0.00461	–

study we derived $(B-V)_0$ intrinsic color index for the eclipsing system as 0.495. The difference between this value and the observed color index is 0.242 and its corresponding temperature and spectral type is 6375 K and F7 (Cox, 2000) respectively which is nearly 142 K lower than the accepted temperature value. In all our solutions, we set the temperature of the hotter component as $T_1 = 6517$ K based on our derived spectral type.

The linear bolometric and logarithmic darkening coefficients were taken from van Hamme (1993). The gravity darkening exponents and the bolometric albedos were set to be 0.32 (Lucy, 1967) and 0.50 (Rucinski, 1969), respectively for both components, because of the convective atmospheres. The grid resolution values were taken to be 40, 30, 15, 15 for N1, N2, N1L and N2L and the detailed reflection model Wilson, 1990 was used with a two reflection (MREF = 2, NREF = 2). A circular orbit and synchronous rotation were assumed which are expected for overcontact binary systems. After a suitable solution was reached, the third light was allowed to vary because on the 2MASS colored images there is a reddish object very close (almost touching) to the binary system. However, the differential corrections did not indicate any significant third light in the system, and so we assume that its contribution is negligible.

For our solutions we assumed that the system is in contact, employing the Mode 3 option of the computing code (overcontact mode). The adjustable parameters for the simultaneous fitting of the light curves were: the inclination i, the mean surface temperature of secondary component T_2, the non-dimensional surface potential of primary component Ω_1 and the monochromatic luminosity of the primary component L_1. Simultaneously, the radial velocity parameters adjusted were: the semi-major axis a, velocity of the center of the mass V_γ and the mass ratio of the system $q = m_2/m_1$. We selected IPB = 0, thus the temperature of the secondary component was used to calculate the L_2 values.

The photometric mass ratio and orbital inclination were determined by Bradstreet et al. (2013) to be $q = 4.148(13)$ and $i = 95^\circ.37(18)$ $(180^\circ - i = 84^\circ.63)$. With the initial parameters (T_2, q_{phot}, i), we solved the light and radial velocity curves simultaneously until the solution converged. The convergent solution was obtained with the adjustable parameters by iterating, until the correction on the parameters became smaller than the corresponding standard deviations. The theoretical light and radial velocity curves calculated with the final elements are shown in Figs. 6 and 7. The results of the final solution are given in Table 9. The configuration of V546 And calculated with the Roche model is shown in Fig. 8.

4. Absolute parameters

Combining the parameters of the photometric and spectroscopic orbital solutions, we derived absolute parameters for the components. Taking the orbital period, $P = 0^d.3830195(43)$, and semi-major axis $a(R_\odot) = 2.458 \pm 0.022$, we can calculate the system's total mass (P in year and a in AU) by using Newton's formulation of Kepler's third law:

$$a^3/P^2 = (M_1 + M_2) = (1.358 \pm 0.037)\,M_\odot \tag{8}$$

According to the light and radial velocity curve solution, the mass ratio of the system is found to be $q = m_2/m_1 = 3.9367 \pm 0.0114$. For the primary and secondary components we derived $M_1 = (0.275 \pm 0.008)\,M_\odot$ and $M_2 = (1.083 \pm 0.030)\,M_\odot$.

The volume radii of the components were estimated with the formula given by Eggleton (1983),

$$r_{VR} = \frac{0.49q^{2/3}}{0.6q^{2/3} + ln(1+q^{1/3})}, \quad 0 < q < \infty \tag{9}$$

and the calculated values are $r_1 = 0.2688 \pm 0.0003$ and $r_2 = 0.5000 \pm 0.0002$ for primary and secondary components respectively. By using the semi-major axis and the volume radius values, we can find the radii of the components in solar units separately. The cal-

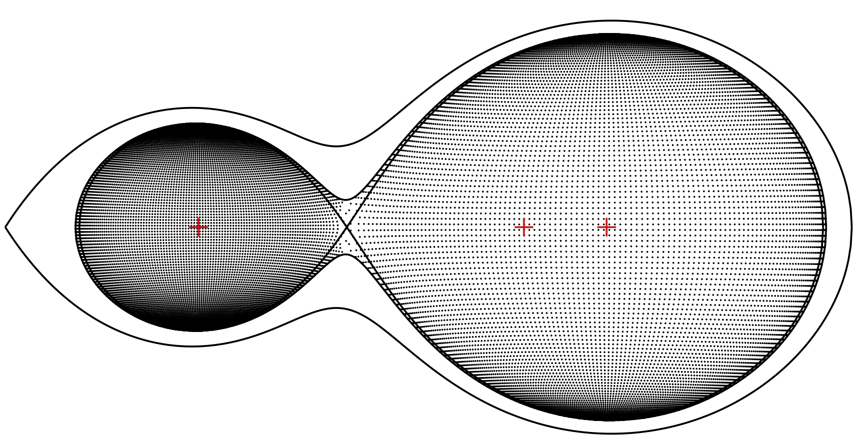

Fig. 8. Roche geometry of the components of V546 And for the orbital phase 0.250.

Table 10
Absolute parameters of V546 And.

Parameters	Primary	Secondary
Mass ($M_\odot$)	0.275 ± 0.008	1.083 ± 0.030
Radius ($R_\odot$)	0.661 ± 0.006	1.229 ± 0.016
Luminosity ($L_\odot$)	0.706 ± 0.045	2.052 ± 0.041
M_{bol}	5.129 ± 0.070	3.969 ± 0.028
Logg (cgs)	4.237 ± 0.014	4.293 ± 0.016
ρ (cgs)	1.344 ± 0.003	0.822 ± 0.002
a ($R_\odot$)	2.458 ± 0.022	
d (pc)	206 ± 1	

culated radii of the components are $R_1 = a \times r_1 = (0.661 \pm 0.006)\ R_\odot$ and $R_2 = a \times r_2 = (1.229 \pm 0.016)\ R_\odot$. Since the sum of the volume radius of the components is $r_{vol.} = r_{1vol} + r_{2vol} = 0.769 > 0.75$ the system is in marginal contact state (Kopal Z., 1959).

The absolute parameters of $M_{bol1,2}$ and $L_{1,2}$ can be calculated using the well-known Eqs. (10) and (11) respectively,

$$M_{bol1,2} = 4^m.75 - 5log(R_{1,2}/R_\odot) - 10log(T_{1,2}/T_\odot), \tag{10}$$

$$L_{1,2} = (R_{1,2}/R_\odot)^2 (T_{1,2}/T_\odot)^4. \tag{11}$$

Adopting $T_\odot = 5780$ K, the bolometric magnitudes are found to be $M_{bol1} = 5.129 \pm 0.070$ and $M_{bol2} = 3.969 \pm 0.028$, and luminosities $L_1 = (0.706 \pm 0.045)\ L_\odot$ and $L_2 = (2.052 \pm 0.041)\ L_\odot$ for the primary and secondary component, respectively. The derived mean densities of the components are $\rho_1 = 1.344 \pm 0.003$ gr/cm^3 and $\rho_2 = 0.822 \pm 0.002$ gr/cm^3, using the equations given below by Mochnacki (1981):

$$\rho_1 = \frac{0.0189}{r^3_{1mean} P^2 (1+q)} \quad and \quad \rho_2 = \frac{0.0189q}{r^3_{2mean} P^2 (1+q)} \tag{12}$$

The spectral type of the hotter and cooler components were found to be as F5 and F7 from the tables given by Cox, 2000.

Because of the total eclipse on the primary minima, we can obtain the magnitude of the secondary component from the light curve, $V_{sec.} = 11^m.573 \pm 0.007$. Using the table of the MK spectral types given in Allen's Astrophysical Quantities (Cox, 2000) for the F5V and F7V spectral types we found the Bolometric Correction (BC) as -0.14 and -0.153 respectively. Since the bolometric magnitude of the secondary component is known (given in Table 10), we can find the absolute magnitude of the component using the formula; $M_{2V} = M_{bol2} - BC = 4^m.037$. The temperature of the secondary component is also known, so we can obtain the intrinsic color $(B-V)_0 = 0.493$ from the tables of Cox (2000). Using this value and the observed color corresponding to the orbital phase 0.0, $(B-V) = 0.737 \pm 0.015$, we can obtain the Color Excess as, $E(B-V) = (B-V) - (B-V)_0 = 0.244 \pm 0.015$, and can find the interstellar extinction in V filter as $A_V = 3.1 \times E(B-V) = 0.756 \pm 0.065$. With those values, we calculate the distance of the primary component (and/or the distance of the system) as,

$$d(pc) = 10^{((V_{sec.} - A_V - M_{sec.V} + 5)/5)} = 206.1 \pm 1.3 \tag{13}$$

The calculated distance to the eclipsing system is close to the value given by Gettel et al. (2006) as $d = 215$ pc. In Table 10 we present the absolute parameters obtained for V546 And.

The location of the components of V546 And on the plot of $LogT - LogL$ is given in Fig. 9, including other A- and W-type W UMa systems obtained from the work of Yakut and Eggleton (2005). The sense of primary and secondary for the systems plotted in Fig. 9 is the reverse of the definition we have selected in our analysis, so we have plotted them in the same sense of Yakut and Eggleton (2005), i.e., the primary star is the more massive star and the secondary is the less massive star. As can be seen in Fig. 9, the primary and secondary components of V546 And are located among the W-type systems.

5. Results and discussions

We derived, for the first time, a combined photometric and spectroscopic solution for the eclipsing binary V546 And. It is found that the binary is a W-type over-contact system with a mass ratio of $q = 3.9367$. The primary eclipse is total and the system has an orbital inclination of $i = 86.07(\pm 0.27)$. The temperature difference between the components is $\Delta T = 277$ K and the individual values correspond to spectral types are approximately F5 and F7 for the primary and secondary. The degree of geometrical contact, defined by the fill-out parameter, $f = (\Omega_{in} - \Omega)/(\Omega_{in} - \Omega_{out})$ is 12.56%, which means that the system is an over-contact binary,

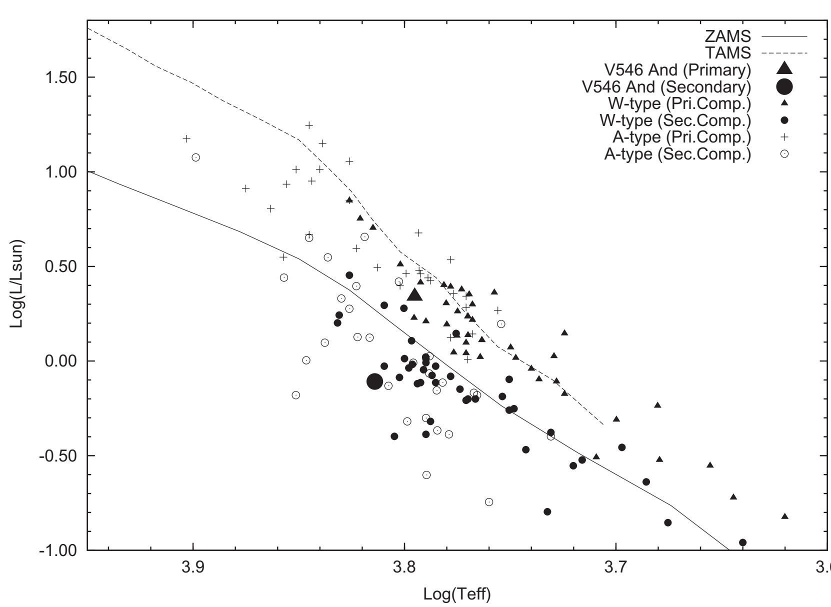

Fig. 9. The location of the components of V546 And in the $LogT - LogL$ diagram. Open symbols for primary and full symbols denote the secondaries. The sample of W- and A-type systems was obtained from Yakut and Eggleton (2005). The lines shown are the solar-metallicity, ZAMS (lower) and TAMS (upper), obtained from Girardi et al. (2000).

and is consistent with the W-type W UMa systems (Dryomova and Svechnikov, 2006).

Acknowledgments

We thank TUBITAK National Observatory (TUG) for a partial support in using RTT150 telescope with project number 10BRTT150–031 and to the observers of the system mentioned in Table 1. This research has made use of the SIMBAD database, operated at CDS, Strasbourg, France, and NASA's Astrophysics Data System Abstract Service. This publication makes use of data products from the Two Micron All Sky Survey, which is a joint project of the University of Massachusetts and the Infrared Processing and Analysis Center/California Institute of Technology, funded by the National Aeronautics and Space Administration and the National Science Foundation. We would like to express our sincere gratitude to the anonymous reviewer for their useful comments which improved the quality of this paper.

References

Applegate, J.H., 1992. ApJ 385, 621.
Binnendijk, L., 1970. Vistas Astron. 12 (1), 217.
Bradstreet, D.H., Sanders, S.J., Volpert, C.G., 2013. Am. Astron. Soc., AAS Meeting 221, 142.
Cox, Arthur N. (Ed.), 2000. Allen's Astrophysical Quantities, fourth ed. Springer-Verlag.
Diethelm, R., 2013. IAU Inform. Bull. Var. Stars 6042.
Dryomova, G.N., Svechnikov, M.A., 2006. Astrophysics 49 (3), 358.
Eggleton, P.P., 1983. ApJ 268, 368.
Fifth Fundamental Catalogue (FK5), 2000.
Gettel, S.J., Geske, M.T., McKay, T.A., 2006. AJ 131, 621.
Girardi, L., Bressan, A., Bertelli, G., Chiosi, C., 2000. A & AS 141, 371.
Gökay, G., Demircan, Y., Gürsoytrak, H., Terzioglu, Z., Okan, A., Dogruel, M.B., Saral, G., Cerit, S., Semuni, M., Kiliç, Y., Çoker, D., Derman, E., Gürol, B., 2012. IAU Inform. Bull. Var. Stars 6039.
Gürol, B., 2005. New Astron. 10, 653.
Gürsoytrak, H., Demircan, Y., Gökay, G., Okan, A., Terzioğlu, Z., Saral, G., Semuni, M., Kılıç, Y., Cerit, S., Alpsoy, M., Yolkolu, A., Sahin, S., Gürol, B., 2013. IAU Inform. Bull. Var. Stars 6075.
Hargis, J.R., Bradstreet, D.H., Lake, J.S., Jewett, F.D., Wilkinson, G.R., Blair, J.M., Guinan, E.F., Ribas, I., McCook, G.P., 2000. BAAS 32, 1480.
Hilditch, R.W., 2001. An Introduction to Close Binary Stars. Cambridge University Press, ISBN 0-521-24106-5.
Hoffman, D.I., Harrison, T.E., McNamara, B.J., 2009. Astron. J. 138, 466.
Honkov K., Juryek J., Lehky M., 67 co-authors, 2013. B.R.N.O. Contributions No. 38, <http://var.astro.cz/oejv/issues/oejv0160.pdf>.
Houdashelt, M.L., Bell, R.A., Sweigart, A.V., 2000. AJ 119, 1448.
Irwin, J.B., 1952. ApJ 116, 211.
Irwin, J.B., 1959. AJ 64, 149.
Kopal Z., 1959. Close Binary Systems, 1959cbs.book....K.
Lucy, L.B., 1967. Z. Astrophys. 65, 89.
Mochnacki, S.W., 1981. ApJ 245, 650.
Nelson, R.H., 2005. Software by Bob Nelson, <http://members.shaw.co/bob.nelson/software1.htm>.
Nelson, Robert H., 2014. IAU Inform. Bull. Var. Stars 6092.
Nicholson, M., Varley, H., 2006. IAU Inform. Bull. Var. Stars 5700 (Report No. 33).
Pickles, A., Depagne, E., 2010. Publ. Astron. Soc. Pac. 122, 1437.
Rucinski, S.M., 1969. Acta Astron. 19, 245.
Rucinski, S.M., 1992. AJ 104, 1968.
Rucinski, S.M., 2002. AJ 124, 1746.
Skrutskie, M.F., Cutri, R.M., Stiening, R., Weinberg, M.D., Schneider, S., Carpenter, J.M., Beichman, C., Capps, R., Chester, T., Elias, J., Huchra, J., Liebert, J., Lonsdale, C., Monet, D.G., Price, S., Seitzer, P., Jarrett, T., Kirkpatrick, J.D., Gizis, J., Howard, E., Evans, T., Fowler, J., Fullmer, L., Hurt, R., Light, R., Kopan, E.L., Marsh, K.A., McCallon, H.L., Tam, R., Van Dyk, S., Wheelock, S., 2006. AJ 131, 1163.
Terrell, D., Wilson, R.E., 2005. Astrophys. Space Sci. 296, 221.
van Hamme, W., 1993. Astron. J. 106, 2096.
Wang, J.M., 1994. ApJ 434, 277.
Wilson, R.E., 1978. ApJ 224, 885.
Wilson, R.E., 1979. ApJ 234, 1054.
Wilson, R.E., 1990. ApJ 356, 613.
Wilson, R.E., Devinney, E.J., 1971. ApJ 166, 605.
Wilson, R.E., Van Hamme, W., 2007. Documentation of Eclipsing Binary Compute Model. Astronomy Department, University of Florida, Gainesville.
Yakut, K., Eggleton, P.P., 2005. ApJ 629, 1055.